OPEN ACCESS

Journal of Statistical Mechanics: Theory and Experiment
An IOP and SISSA journal

PAPER: Classical statistical mechanics, equilibrium and non-equilibrium

The simplified energy landscape of the ϕ^4 model and the phase transition

Fabrizio Baroni

IFAC-CNR Institute of Applied Physics 'Nello Carrara', Sesto Fiorentino (FI), Italy
E-mail: f.baroni@ifac.cnr.it and baronifab@libero.it

Received 20 February 2024
Accepted for publication 29 May 2024
Published 10 July 2024

CrossMark

Online at stacks.iop.org/JSTAT/2024/073201
https://doi.org/10.1088/1742-5468/ad5437

Abstract. The on-lattice ϕ^4 model is a paradigmatic example of a continuous real-variable model undergoing a continuous symmetry-breaking phase transition (SBPT). Here, we study the $\mathbb{Z}_2$-symmetric mean-field case without the quadratic term in the local potential. We show that the $\mathbb{Z}_2$-SBPT is not affected by the quadratic term and that the potential energy landscape is greatly simplified from a geometric–topological viewpoint. In particular, only three critical points exist to confront, with a number growing as e^N (N is the number of degrees of freedom) of the model with a negative quadratic term. We focus on the properties of the equipotential surfaces with the aim to deepen the link between SBPTs and the essential properties of a potential that is capable of entailing them. The results are interpreted in view of of some recent achievements regarding rigorous necessary and sufficient conditions for a $\mathbb{Z}_2$-SBPT.

Keywords: phase transitions, energy landscape, configuration space, symmetry breaking

Contents

1. Introduction

This study is part of a research line attempting to clarify the relationship between phase transitions (PTs) and the potential energy landscapes of Hamiltonian systems (for example, see [1–12]). Potential landscapes include critical points, geometric properties and the topology of suitable subsets of configuration space, for example, equipotential surfaces. This type of study often makes intensive use of models undergoing PTs, including the ϕ^4 model. This model has received increasing attention in recent years, and is a paradigmatic example of a model undergoing a continuous PT (for example, see [6, 13–22]). Here, we introduce a simplified version of the model that shows a reduced number of critical points compared with the traditional version.

The ϕ^4 model is a lattice version of a classical ϕ^4 field model. This can be studied in any spatial dimension, in scalar and vector versions by the Hamiltonian

$$H = \sum_{\alpha=1}^{n} \sum_{i=1}^{N} \left[\frac{1}{2} (\pi_i^\alpha)^2 - \frac{\mu}{2} (\phi_i^\alpha)^2 - J \sum_{\langle i,j \rangle} \phi_i^\alpha \phi_j^\alpha \right] + \frac{\lambda}{4} \sum_{i=1}^{N} \left[\sum_{\alpha=1}^{n} (\phi_i^\alpha)^2 \right]^2, \tag{1}$$

where the index α runs from 1 to n for an $O(n)$ symmetry group, the index i labels the d-dimensional spatial lattice, (π_i, ϕ_i) are the canonically conjugated variables, N is the number of degrees of freedom and $\langle i,j\rangle$ is the set of the nearest-neighbor lattice sites of the ith site [23]. The set $\langle i,j\rangle$ can be defined in other ways, for example, the set of all the variables within a certain range, or the whole lattice in mean-field interactions.

The model is known to undergo an $O(n)$-symmetry-breaking PT (SBPT). The existence of an SBPT can be proven by using renormalization group arguments [24]. For $d=2$ and $n=2$, and according to the Mermin–Wagner theorem, the model cannot have any SBPT because of the combination of short-range interactions, continuous symmetry and two spatial dimensions. In fact, it undergoes a Kosterlitz–Thouless PT without affecting the order parameter, which remains vanishing, even below the critical temperature.

In [15], the topology of the equipotential surfaces interior of the mean-field ϕ^4 model of an $O(1)$ symmetry (also called $\mathbb{Z}_2$) was solved using Morse theory. A large number of critical points that exponentially increase with N were identified. In [6, 20], a similar study was conducted using the nearest-neighbor 2D version. At sufficiently small values of the coupling J, there is no difference in the number of critical points compared to the mean-field version, but by increasing J and leaving fixed N, their number rapidly drops to only three.

To simplify the following studies, we define the *local potential* V_{loc} of the Hamiltonian (1) as the additive part of the potential, which depends only on the degrees of freedom of a single lattice site

$$V_{\mathrm{loc}} = \sum_{\alpha=1}^{n} \left(\frac{\lambda}{4} \left[(\phi^\alpha)^2 \right]^2 - \frac{\mu}{2} (\phi^\alpha)^2 \right). \tag{2}$$

In this study, we found the negative quadratic term in the local potential of the mean-field ϕ^4 model with a $\mathbb{Z}_2$ symmetry to be responsible for the rapid growth of the number of critical points while increasing N. Knowing this, we ask if the presence of the quadratic term can be justified to entail the $\mathbb{Z}_2$-SBPT. Firstly, it is derived from classical field theory, where it is the mass term of the associated classical field; for this reason, it is often labeled as $\mu^2>0$. Another reason to justify the presence of the negative quadratic term is the wish to simulate the classical spin of the Ising model. Indeed, for $n=1$, the ϕ^4 model can be seen as a continuous-variable version of the classical Ising model, whose classical spins, S_i's, can take only two values: generically assumed as ± 1. In the ϕ^4 model with a $\mathbb{Z}_2$ symmetry, the role of the two permitted values of the S_i's are played by the two global minima of the double-well local potential $V_{\mathrm{loc}}(\phi) = \lambda\phi^4 - \mu\phi^2$ entailed by the negative quadratic term.

There is a remarkable difference between the S_i's and the ϕ_i's: the former do not find any resistance at jumping between the two permitted values, whereas the latter find such a resistance at jumping between the two global minima because of the presence of the potential barrier. Hence, in our opinion, the double well introduces a complication which is not present in the classical Ising model; furthermore, it is not even necessary to entail the $\mathbb{Z}_2$-SBPT. For these reasons, in the following we allow μ to be vanishing or, in some particular conditions, negative.

In section 2, we set μ to zero in the mean-field version of the ϕ^4 model with a $\mathbb{Z}_2$ symmetry because it is the simplest case with both canonical thermodynamic and critical points of configuration space that are solvable in a semi-analytical way. In section 3, we study the same model without an interacting potential, where no SBPT occurs in order to make a comparison. In section 4, we consider some short-range versions and find all their critical points by using the numerical polynomial-homotopy-continuation (NPHC) method up to $N = 9$.

2. Mean-field $\mathbb{Z}_2$-symmetric ϕ^4 model with a vanishing quadratic term in the local potential

Here, we disregard the kinetic terms $\pi_i^2/2$, $i = 1, \ldots, N$, in the Hamiltonian, equation (1), because they yield a trivial contribution to the partition function, which can be factorized. From a topological viewpoint, the level sets at constant kinetic energy in phase space are trivially equivalent to N-spheres. Then, we set the parameters $\lambda = 2/N$, $\mu = 0$ and extend the interaction to all the pairs of coordinates (i.e. mean-field interaction) giving rise to the potential

$$V = \sum_{i=1}^{N} \frac{1}{4}\phi_i^4 - \frac{J}{2N}\left(\sum_{i=1}^{N}\phi_i\right)^2. \tag{3}$$

2.1. Canonical thermodynamic

In [15, 25], the thermodynamic of the model, equation (1), with $\lambda = 2/N$, $\mu = 1$ and mean-field interactions

$$V = \sum_{i=1}^{N}\left(\frac{1}{4}\phi_i^4 - \frac{1}{2}\phi_i^2\right) - \frac{J}{2N}\left(\sum_{i=1}^{N}\phi_i\right)^2 \tag{4}$$

was solved using mean-field theory. In this section, we will follow the same pathway for the model, equation (3). In figures 1 and 2, the results for these two models are compared.

The configurational partition function is

$$Z = \int \mathrm{d}^N\phi\, \mathrm{e}^{-\beta\left[\sum_{i=1}^{N} V_{\mathrm{loc}}(\phi_i) - \frac{J}{2N}\left(\sum_{i=1}^{N}\phi_i\right)^2\right]}, \tag{5}$$

where $V_{\mathrm{loc}}(\phi) = \phi^4/4$ is the local potential of the potential, equation (3), defined in equation (2), and $\beta = 1/T$. We introduce the magnetization

$$m = \frac{1}{N}\sum_{i=1}^{N}\phi_i, \tag{6}$$

which, replaced in Z, gives

$$Z = \int \mathrm{d}^N\phi\, \mathrm{e}^{-\beta\left[\sum_{i=1}^{N} V_{\mathrm{loc}}(\phi_i) - \frac{JN}{2}m^2\right]}. \tag{7}$$

The fact that the mean-field interactions imply that the interacting potential is a function of the magnetization, allows us to solve Z in a semi-analytic way using the Hubbard–Stratonovich transformation [15, 25, 26] based on the Gaussian integral

$$\mathrm{e}^{\mu m^2} = \frac{1}{\sqrt{\pi}} \int \mathrm{d}y\, \mathrm{e}^{-y^2 + 2\sqrt{\mu} m y}, \tag{8}$$

which, inserted into equation (7), yields

$$Z = \frac{1}{\sqrt{\pi}} \int \mathrm{d}y \left[\int \mathrm{d}\phi\, \mathrm{e}^{-\beta V_{\mathrm{loc}}(\phi) + \sqrt{\frac{2\beta J}{N}} m\phi} \right]^N \mathrm{e}^{-y^2}. \tag{9}$$

After introducing

$$\varphi(m, \beta) = \ln \int \mathrm{d}q\, \mathrm{e}^{-\beta[V_{\mathrm{loc}}(q) + Jmq]}, \tag{10}$$

and the variable changing $y = \sqrt{\frac{N\beta J}{2}} m$, we get

$$Z = \sqrt{\frac{N\beta J}{2\pi}} \int \mathrm{d}m\, \mathrm{e}^{-N\beta f(m,\beta)}, \tag{11}$$

where

$$f = -\frac{J}{2} m^2 + \frac{1}{\beta} \varphi(m, \beta) \tag{12}$$

is the configurational Helmholtz free energy per degree of freedom.

Finally, to apply the saddle-point method to calculate Z, we minimize f with respect to m at fixed T, obtaining the spontaneous magnetization $\langle m \rangle (T)$. From the latter, we get the specific free energy, the specific average potential and the specific heat

$$f(T) = -\frac{1}{N\beta} \ln Z, \tag{13}$$

$$\langle v \rangle (T) = -\frac{1}{N} \frac{\partial}{\partial \beta} Z, \tag{14}$$

$$c_v(T) = \frac{\mathrm{d}\langle v \rangle}{\mathrm{d}T}, \tag{15}$$

respectively. They are plotted in figure 1 in comparison with the results for the mean-field ϕ^4 model, equation (4). The picture is the well-known one of a second-order $\mathbb{Z}_2$-SBPT with classical critical exponents.

We cannot see any difference in the thermodynamic of the two models, apart from a quantitative viewpoint. We conclude that the negative quadratic term in the local potential has no part in causing the $\mathbb{Z}_2$-SBPT. This is not surprising because in [7],

J. Stat. Mech. (2024) 073201

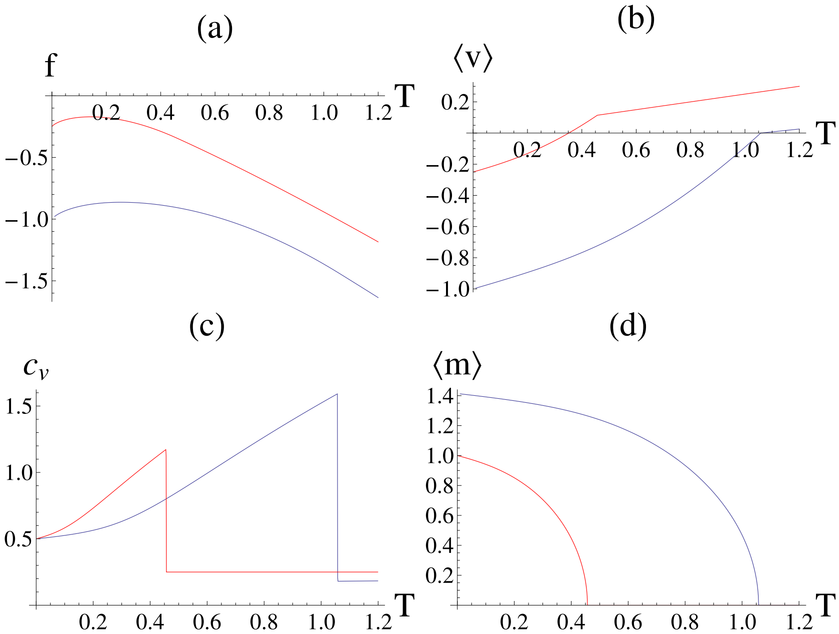

Figure 1. (a)–(d) The specific free energy, average specific potential, specific heat and spontaneous magnetization, respectively, as functions of the temperature. The red lines represent the model in equation (3) and the blue lines represent the model in equation(4), both with the coupling constant $J = 1$.

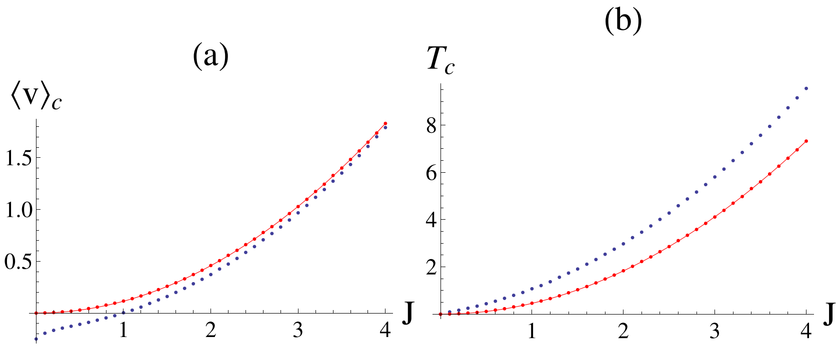

Figure 2. (a) The critical average potential as a function of the coupling constant of the model in equation (3) (red points) and of the model in equation (4) (blue points). The continuous line is the parabola $0.114446J^2$ fitted to the data. (b) As panel (a) for the critical temperature. The continuous line is the parabola $0.457786J^2$.

it was showed that, in a mean-field model, a double-well potential with a minimum barrier between the wells proportional to N is a sufficient condition for entailing a $\mathbb{Z}_2$-SBPT. Both models, equations (3) and (4), have this feature independently of the presence of the quadratic term $-\phi^2/2$ in the local potential. Rather, as we will see in the following, the latter yields complication and confusion about the real link between the characteristics of the potential energy landscape and the $\mathbb{Z}_2$-SBPT.

https://doi.org/10.1088/1742-5468/ad5437

J. Stat. Mech. (2024) 073201

The occurrence of the double well of the potential is generated by the competition between the confining part given by the local potential and the interacting part for $J>0$. The only essential condition to satisfy in order to make the total potential confining is the following

$$\lim_{\phi\to+\infty}\frac{V_{\text{loc}}(\phi)}{\phi^2}=+\infty. \tag{16}$$

For example, let us consider the local potential given by the square well

$$V_{\text{loc}}=\begin{cases}+\infty & \text{for } |\phi|\geqslant 1\\ 0 & \text{for } |\phi|<1\end{cases}, \tag{17}$$

which is nothing but the limit of $V_{\text{loc}}=\phi^{2k}$ for $k\to\infty$ with k natural. With this choice, we get, in the thermodynamic limit, the configurational partition function of the mean-field Ising model, whose free energy is given by

$$f(m,T)=-\frac{J}{2}m^2+1+T\ln\cosh\left(\frac{Jm}{T}\right). \tag{18}$$

From the latter, by setting the derivative to zero with respect to m, we get the well-known spontaneous magnetization as the solutions of the following equation

$$-m+\tanh\left(\frac{Jm}{T}\right)=0. \tag{19}$$

The critical temperature is $T_c=J$.

In [18], large deviation theory was applied to find the configurational microcanonical entropy $s(v,m)$ of the model in equation (4), and of the same model without interaction. We recall the definition of configurational entropy

$$s(v,m)=\lim_{N\to\infty}\frac{1}{N}\ln\omega(v,m), \tag{20}$$

where $\omega(v,m)$ is the density of states at fixed v and m

$$\omega_N(v,m)=\int_{\Sigma_{v,N}\cap\Sigma_{m,N}}\frac{d\Sigma}{\|\nabla V\wedge\nabla M\|}, \tag{21}$$

where $\Sigma_{v,N}$ is defined in equation (25), $\Sigma_{m,N}$ is defined in a similar way for the magnetization, $V=Nv$, $M=Nm$ and $\|\nabla V\wedge\nabla M\|$ is the Gram determinant square root.

Large deviation theory can be applied to the model in equation (3) as well. We expect no qualitative difference in the properties of $s(v,m)$, which is analytic and non-concave. The non-concavity is allowed by the long-range interactions and is strictly related to the SBPT, whereas it is forbidden in the short-range case [19, 27–29]. In simple terms, an equilibrium configuration of a short-range system in the broken symmetry phase can be divided by a layer into two domains, each with magnetization oriented independently of the other. This is made possible because the potential energy at the layer becomes negligible compared with the total one in the thermodynamic limit. Here, we limit

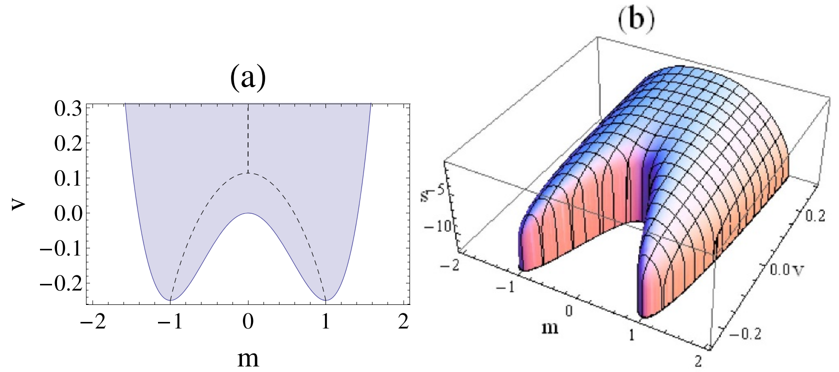

Figure 3. (a) The domain of the configurational entropy s, equation (20), of the model, equation (3) (dark region) in the (m, v)-plane. The dashed line is the spontaneous magnetization, where s takes the maximum evaluated along straight lines with constant v. (b) A 3D plot of s only in qualitative accordance with the real graph of the model, equation (3). The domain is exact.

to give the domain of $s(v,m)$, whose contour $v(m) = m^4/4 - Jm^2/2$ is given by the potential evaluated on the straight line in configuration space passing by the origin of coordinates and orthogonal to the hyperplanes at constant m. The contour is plotted in figure 3.

2.2. Critical points and topology of the equipotential surfaces

Here, $\nabla V = 0$ for the potential, equation (3), takes the form

$$\phi_i^3 - \frac{J}{N}\sum_{i=1}^{N}\phi_i = 0 \qquad i = 1, \ldots, N. \tag{22}$$

The form of the system, equation (22), implies that the components of the solutions are all equal, so that it reduces to $\phi_i^3 - J\phi_i = 0$, $i = 1, \ldots, N$. Trivially, the solutions are $\phi_0^s = (0, \ldots, 0)$ and $\phi_\pm^s = \pm\sqrt{J}\,(1, \ldots, 1)$.

The equipotential surfaces, or v-level sets, are often called $\Sigma_{v,N}$'s in the literature, and are defined as follows

$$\Sigma_{v,N} = \left\{\phi \in \mathbb{R}^N : \frac{V(\phi)}{N} = v\right\}. \tag{23}$$

To apply Morse theory [30], it is useful to also define $M_{v,N}$ as

$$M_{v,N} = \left\{\phi \in \mathbb{R}^N : \frac{V(\phi)}{N} \leqslant v\right\}. \tag{24}$$

Trivially, the $\Sigma_{v,N}$'s are the boundary of the $M_{v,N}$'s

$$\Sigma_{v,N} = \partial M_{v,N}. \tag{25}$$

The topology of the $\Sigma_{v,N}$'s is strictly related to that of the $M_{v,N}$'s.

According to Morse theory, the topology of the $M_{v,N}$'s can be determined by starting from a Morse function defined on configuration space. A Morse function is a function whose critical points are non-degenerate, i.e. isolated. In this case, we use the potential as a Morse function. Once the critical points have been found, the topology of the $M_{v,N}$'s is retrieved by attaching a k-handle $\mathtt{H}^{N,k}$ for each critical point, where N is the configuration space dimension and k is the index of the critical point ($0 \leqslant k \leqslant N$). Here, $\mathtt{H}^{N,k}$ is the product of two disks, one k-dimensional and the other $(N-k)$-dimensional

$$\mathtt{H}^{N,k} = D^k \times D^{N-k}. \tag{26}$$

The index of a critical point is defined as the number of negative eigenvalues of the Hessian matrix H, which, for the potential, equation (3), takes the form

$$H_{ij} = \frac{\partial^2 V}{\partial\phi_i \partial\phi_j} = 3\phi_i^2 \delta_{ij} - \frac{J}{N}. \tag{27}$$

The fact that the critical points are non-degenerate are equivalent to requesting that each critical point is non-singular or, basically, that the determinant of the Hessian matrix is non-vanishing. For $\phi_\pm^s$, $H_{ij} = 3J\delta_{ij} - J/N$. This entails that the index is 0 because all the eigenvalues are positive. For ϕ_0^s, $H_{ij} = -J/N$. This entails that the saddle is singular. Regardless, the saddle is isolated, and here we show that it corresponds to a critical point with index 1. Consider an orthonormal coordinate system, such that an axis is the line passing through the points $\phi_\pm^s$ and the remaining axes are orthogonal to the latter. The second derivative of V along the aforementioned axis computed at ϕ_0^s is negative. The restriction of V on each of the other axes has a global minimum in ϕ_0^s. From these two considerations, we can infer that ϕ_0^s corresponds to a critical point with index 1.

The critical points $\phi_\pm^s$ correspond to the global minimum of the potential $v_{\min} = -J^2/4$ to which the first critical v-level set starting from the bottom corresponds. The saddle ϕ_0^s corresponds to the critical 0-level set, i.e. the second and last critical v-level set from bottom to top. The topologies of the $M_{v,N}$'s are retrieved by attaching two 0-handles $\mathtt{H}^{N,0}$ at the first critical v-level set and a 1-handle $\mathtt{H}^{N,1}$ at the second critical v-level set. Therefore, the $M_{v,N}$'s are homeomorphic to a couple of disjointed N-balls for $v \in (-J^2/4, 0)$, whereas for $v \in (0, +\infty)$, they are homeomorphic to a single N-ball. Equivalently, the topology of the $\Sigma_{v,N}$'s is that of two N-spheres for $v \in (-J^2/4, 0)$ and of an N-sphere for $v \in (0, +\infty)$ (see figure 4).

2.2.1. Interpretation of the results. In [15], the critical points of the model in equation (4) were found by using the same semi-analytic method applied in section 2.1. Figure 5 shows the number of critical points and their density with respect to the

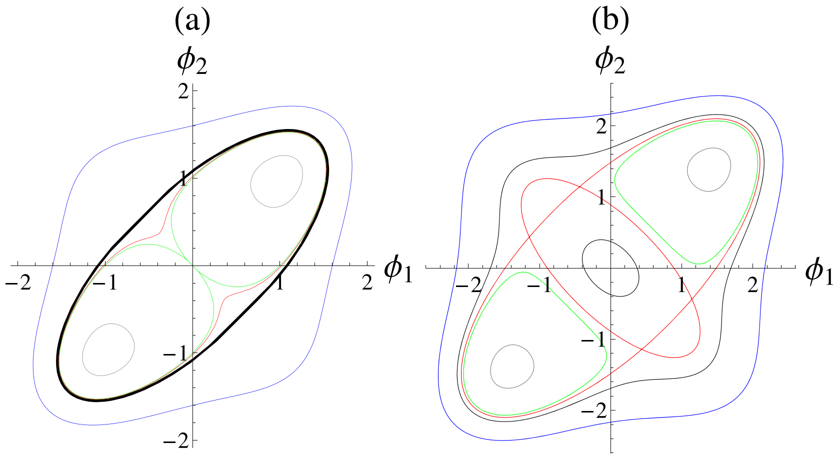

Figure 4. Some $\Sigma_{v,N}$'s of the model, equation (3), (panel (a)) for $N=2$ with $J=1$ in comparison with some of the model in equation (4) (panel (b)). The proliferation of the critical points in the model in equation (4) is already evident at $N=2$. In (a), the bold $\Sigma_{v,N}$ is the precursor of the $\Sigma_{v,N}$ which, for any N, is the boundary between the *dumbbell-shaped* ones and those which are not.

potential density. The total number is of the order of e^N, at least for the J-values investigated, always less or equal to 1. We cannot exclude that, by increasing J with fixed N, a decrease in the number of critical points can occur, similarly to what was detected in [6] for the short-range case. The critical points are comprised between a minimum v-value, significantly greater than the global minimum, and $v=0$. In [15], it was also shown via an analytic demonstration that there are no critical points above $v=0$.

From a viewpoint of the $\Sigma_{v,N}$'s topology, the interval of v-values containing the critical points works as a transition interval between two N-spheres and a single N-sphere (see figures 4 and 6). In the model, equation (3), this transition interval collapses in a single critical v-level set with a single critical point. It is notable that, despite this dramatic simplification of the potential landscape, the model in equation (3) does not lose any properties from a PT viewpoint.

In [16, 31], it was shown that a $\mathbb{Z}_2$-SBPT can be entailed by *dumbbell-shaped* $\Sigma_{v,N}$'s. Roughly speaking, such a $\Sigma_{v,N}$ is made up of two major lobes connected by a narrow neck (see figures 4, 6 and 7). In more detail, a $\Sigma_{v,N}$ is dumbbell-shaped when the microcanonical volume of the section at constant m does not take the global maximum at $m=0$. The critical potential corresponds to the transition between the dumbbell-shaped $\Sigma_{v,N}$'s and those that are not. This $\mathbb{Z}_2$-SBPT generating mechanism was discovered in several models [7, 8, 14, 16, 31, 32] and it is also acting in the models in equations (3) and (4). The picture is represented in figure 7. The method used in section 2.1 to solve the canonical thermodynamic decomposes the N-dimensional integral of the partition function in a one-dimensional integral with respect to m. In this way, the problem to find the microcanonical volume of the sections of the $\Sigma_{v,N}$'s at constant m was solved.

We remark that being dumbbell-shaped for a $\Sigma_{v,N}$ can be independent at all on its critical points and topology. Regardless, there is a special case that is worth mentioning,

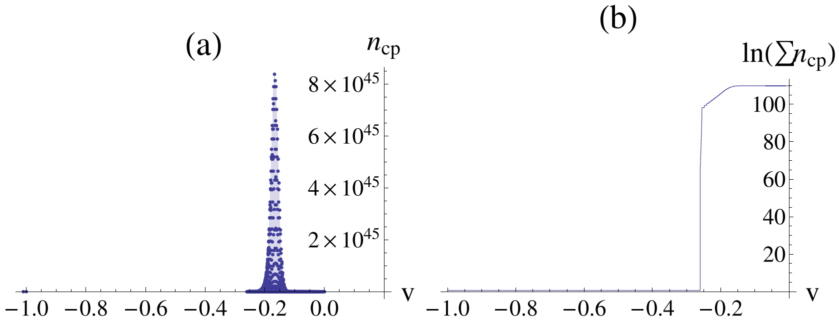

Figure 5. Model (4) for $N = 100$ and $J = 1$. (a) The number of critical points ($n_{\rm cp}$) with respect to their potential density. (b) The logarithmic sum of critical points starting from left versus potential density.

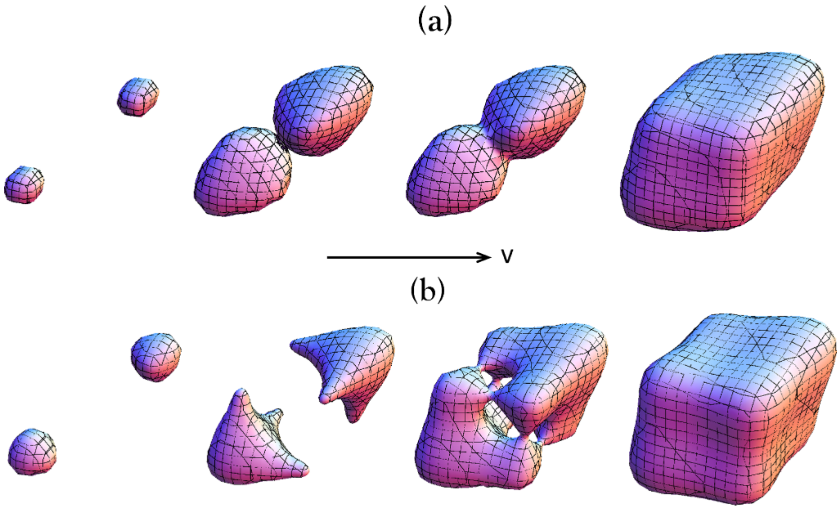

Figure 6. (a) Some $\Sigma_{v,N}$'s of the model, equation (3), for $N = 3$ and $J = 1$. The potential density increases from left to right. (b) The same as (a) for the model in equation (4). In the latter case, the proliferation of the critical points is evident.

i.e. when the $\Sigma_{v,N}$ is made up from two or more connected components which do not intersect the hyperplane at $m = 0$. In this case, the $\Sigma_{v,N}$ is necessarily dumbbell-shaped for obvious reasons. This is the case of the model in equation (3) for v comprised between the global minimum and $v = 0$ and of the model in equation (4) for v comprised between the global minimum and the minimum v-value of the critical $\Sigma_{v,N}$'s. In fact, the $\Sigma_{v,N}$'s are all homeomorphic to two N-spheres.

The fact that a dumbbell-shaped $\Sigma_{v,N}$ implies the $\mathbb{Z}_2$-symmetry breaking has a remarkable consequence on the critical potential $\langle v\rangle_{\rm c}$. In particular, $\langle v\rangle_{\rm c}$ has to be greater than zero for the model in equation (3) and greater than the minimum of the v-values of the critical $\Sigma_{v,N}$'s for the model in equation (4). Both the inferences are compatible with the results obtained here and in [15].

The, $\langle v\rangle_{\rm c} > 0$ is a consequence of theorem 1 in [14], which states that if the $\Sigma_{v,N}$'s are made up of two, or more, disjointed connected components non-intersecting the

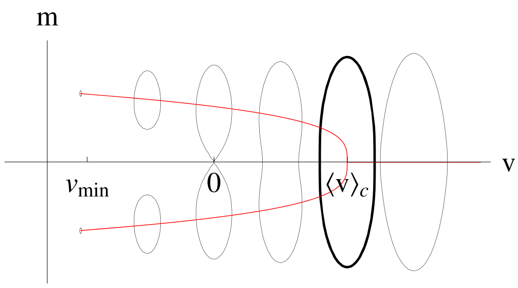

Figure 7. Conceptual representation of the $\mathbb{Z}_2$-symmetry-breaking mechanism based on dumbbell-shaped equipotential surfaces for the model in equation (3). The dumbbell-shaped surfaces are below the thermodynamic critical potential $\langle v\rangle_{\rm c}$. The bold line represents the separating surface with respect to the non-dumbbell-shaped ones above $\langle v\rangle_{\rm c}$. The spontaneous magnetization as a function of potential density is shown in red.

hyperplane at $m=0$ below a certain value v_0 of the potential density, then the $\mathbb{Z}_2$ symmetry is broken for any $v<v_0$. In the model in equation (3), $v_0=0$. This condition is a special case of the sufficient condition given in theorem 1 in [16] based on dumbbell-shaped $\Sigma_{v,N}$'s. This is because if the $\Sigma_{v,N}$'s are made up as just described above, the more likely they are also dumbbell-shaped.

3. Model (3) without interaction

To make a comparison with a model without SBPT, the interacting terms were removed from the potential, equation (3)

$$V=\frac{1}{4}\sum_{i=1}^{N}\phi_i^4. \tag{28}$$

The solution of the canonical thermodynamic is trivial because the system is nothing but a collection of N independent quartic oscillators. No PT can occur. The configurational partition function is given by

$$Z=\left(\int \mathrm{d}\phi\, \mathrm{e}^{-\frac{1}{4}\beta\phi^4}\right)^N=\left(\frac{\gamma\left(\frac{1}{4}\right)}{\sqrt{2}}T^{\frac{1}{4}}\right)^N, \tag{29}$$

from which we get the caloric curve $\langle v\rangle(T)=T/4$.

The topology of configuration space is even more trivial. Indeed, $\nabla V=0$ takes the simple form

$$\phi_i^3=0 \qquad i=1,\dots,N, \tag{30}$$

whose unique solution is $(0,\dots,0)$. The index cannot be computed as for a Morse function because the Hessian matrix vanishes at $(0,\dots,0)$. However, since $(0,\dots,0)$ is a

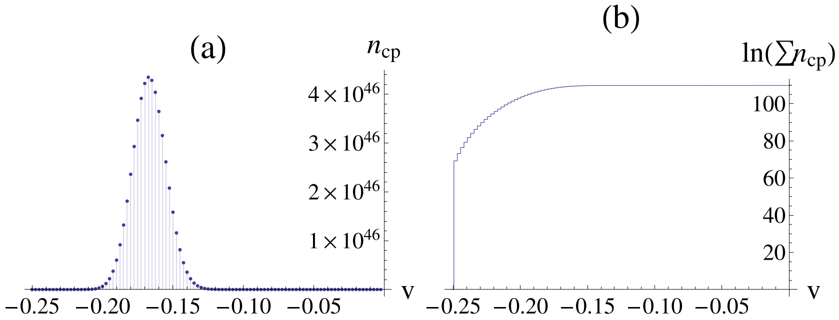

Figure 8. Model (4) without interacting terms for $N = 100$. (a) The number of critical points (n_{cp}) with respect to their potential density. (b) The logarithmic sum of the number of critical points starting from left versus potential density.

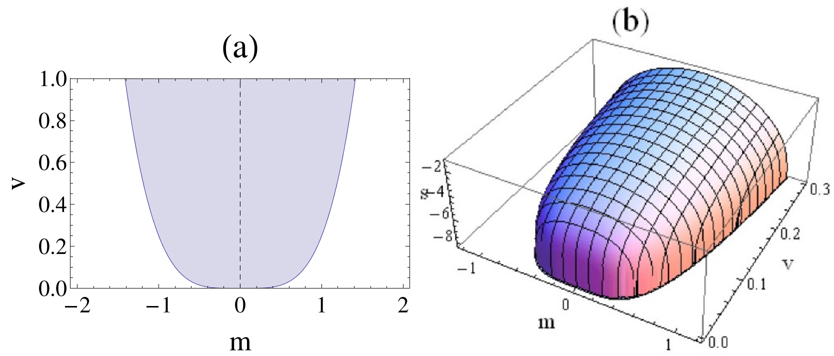

Figure 9. (a) The domain of the configurational entropy s, equation (20), of the model in equation (28) (dark region) in the $(m,\ v)$-plane. The dashed line is the spontaneous magnetization, where s takes the maximum evaluated along straight lines with constant v. (b) A 3D plot of s only in qualitative accordance with the real graph of the model in equation (28). The domain is exact.

global minimum, it corresponds to a non-singular stationary point with index 0. From a topological viewpoint, the topology of the $M_{v,N}$'s, for $v > 0$, can be retrieved by attaching a 0-handle $\mathtt{H}^{0,N}$ at the 0-level set. Hence, the $M_{v,N}$'s are homeomorphic to an N-ball for $v > 0$. The model cannot undergo any SBPT, not even at $T = 0$, because at that temperature the representative point is frozen at $(0, \ldots, 0)$ to which a vanishing spontaneous magnetization corresponds.

For comparison with the model in equation (28), in figure 8 we show the critical points of the model in equation (4) without the interaction investigated in [15]. The total number of critical points is 3^N, which is entirely due to the presence of the negative quadratic term in the local potential. Here, 3^N comes from the combinatorial of the three solutions of the third-degree equations inside the system $\nabla V = 0$.

In figure 9, we report the graphic of the configurational microcanonical entropy, which is strictly concave, as it is in a system without SBPT.

4. Short-range case

Here, we conjecture that the models of the class in equation (1) without a quadratic in the local potential still have a PT of the same type. We have no general demonstration available, but we provide some evidence that makes this conjecture very reasonable.

In this section, we will investigate the nearest-neighbor-interaction version of the mean-field simplified ϕ^4 model in equation (3) introduced in section 2. The potential is the following

$$V = \frac{1}{4}\sum_{i=1}^{N}\phi_i^4 - J\sum_{\langle i,j\rangle}\phi_i\phi_j, \tag{31}$$

where we assume toroidal boundary conditions and $J > 0$. The lattice can have any dimension d.

4.1. Canonical thermodynamic

By analysis, we can compute only the value of the spontaneous magnetization and of the specific potential at $T = 0$. By inserting $q_i = q_0$, for $i = 1, \ldots, N$, in equation (31) and dividing by N, we obtain

$$v = \frac{1}{4}q_0^4 - dJq_0^2, \tag{32}$$

from which, by vanishing the derivative

$$\frac{\partial v}{\partial q_0} = q_0^3 - 2dJq_0 = 0, \tag{33}$$

we get the solution of the spontaneous magnetization $q_0 = 0, \pm\sqrt{2dJ}$ and of the specific potential $v_{\mathrm{min}} = -d^2J^2$. Here, $q_0 = 0$ has to be excluded for obvious reasons.

Some Monte Carlo simulations were carried out while varying d and J. For $J = 1$, the lattice dimensions are $d = 1, 2, 3, 4$ with nearest-neighbors interaction, periodic boundary conditions for $d = 1$ and toroidal boundary conditions for the other d-values. For $d = 2$, the coupling constant is $J = 0.5, 1, 1.5, 2$. The results are shown in figure 10. As expected, the model shows a second-order PT, except for $d = 1$, where the PT occurs at $T = 0$. In general, we conjecture that the model in equation (31) undergoes a $\mathbb{Z}_2$-SBPT for any d and for any $J > 0$, and belongs to the universality class of the classical Ising model in d dimension, even extending the range of the interaction not only at nearest neighbors. Among the $\mathbb{Z}_2$-SBPTs, we also include the special case $d = 1$ as a limiting case with the critical temperature $T_{\mathrm{c}} = 0$.

Despite the difficulty associated with the precise estimation of the critical temperature T_{c} and the critical potential $\langle v\rangle_{\mathrm{c}}$ as functions of d and J by those simulations, a quadratic relationship seems very reasonable. The rise of the minimum barrier between the two wells of the potential by increasing d and J explains the increase in T_{c} and $\langle v\rangle_{\mathrm{c}}$. The simulations suggest $\langle v\rangle_{\mathrm{c}} > 0$ for any d and $J > 0$.

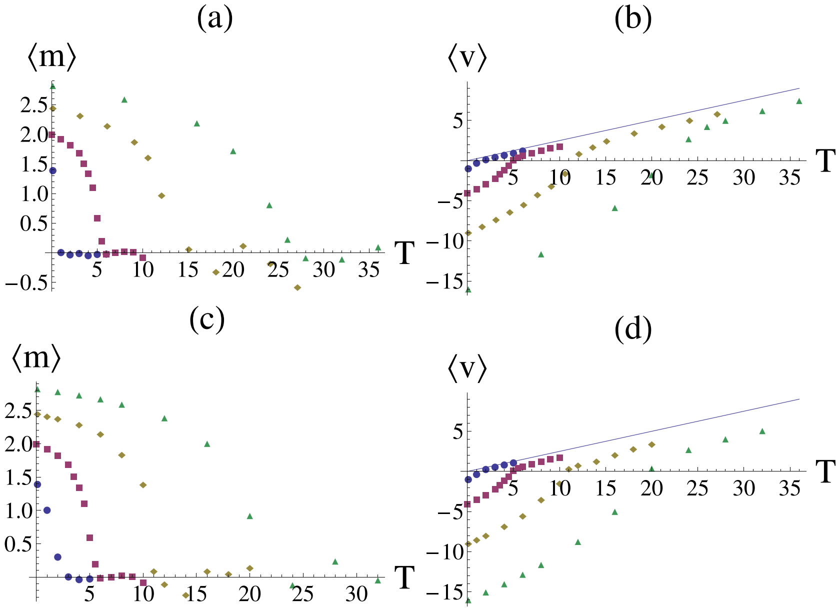

Figure 10. (a) Monte Carlo simulations for the spontaneous magnetization as a function of the temperature of the model in equation (31) for $J = 1$. Disks are for $d = 1$ and $N = 100$, squares are for $d = 2$ and a 10×10 lattice, rhombuses are for $d = 3$ and a $4 \times 4 \times 4$ lattice, triangles are for $d = 4$ and a $3 \times 3 \times 3 \times 3$ lattice. (b) The same as (a) for the specific potential. The continuous line $T/4$ is for the model without interaction. (c) The same as (a) for $d = 2$ and a 10×10 lattice with $J = 0.5, 1, 1.5, 2$ for disks, squares, rhombuses and triangles, respectively. (d) The same as (c) for the specific potential.

4.2. Critical points and topology of the equipotential surfaces

Here, $\nabla V = 0$, for the potential in equation (31), takes the form

$$\phi_i^3 - J \sum_{\langle i,j \rangle} \phi_j = 0 \qquad i = 1, \ldots, N. \tag{34}$$

A remarkable property, for any lattice dimension d, is the existence of a scaling law that links the critical points evaluated at different values of the coupling J. The scaling is as follows

$$\begin{cases} J \to J' \\ \phi_i \to \phi_i' = k\phi_i \qquad i = 1, \ldots, N \\ m \to m' = km \\ v \to v' = k^4 v \end{cases}, \tag{35}$$

J. Stat. Mech. (2024) 073201

where $k=\sqrt{J'/J}$. To prove it, consider

$$k^3\left(\phi_i^3 - Jk^{-2}\sum_{\langle i,j\rangle}\phi_j\right)=0 \qquad i=1,\ldots,N. \tag{36}$$

It is immediate to verify that if the set of coordinated ϕ_i, $i=1,\ldots,N$, is a critical point, then the new set $k\phi_i$, $i=1,\ldots,N$, is a solution of $\nabla V=0$ for J'. The scaling also holds for the mean-field case.

In [15], it was analytically proven that all the critical levels of the model in equation (4) are below zero. Here, we extend the demonstration to the model in equation (31). From equation (34), we deduce that if $\boldsymbol{\phi}^s$ is a stationary point, then

$$(\phi_i^s)^3 = J\sum_{\langle i,j\rangle}\phi_j^s \qquad i=1,\ldots,N. \tag{37}$$

Rewriting the potential in equation (31) in the following form

$$V=\sum_{i=1}^{N}\phi_i\left(\frac{1}{4}\phi_i^3 - J\sum_{\langle i,j\rangle}\phi_j\right), \tag{38}$$

and substituting equation (37), we get

$$V(\phi^s) = -\frac{3}{4}\sum_{i=1}^{N}(\phi_i^s)^4\leqslant 0. \tag{39}$$

To deepen a relationship with critical points and a thermodynamic, let us define the minimum barrier $B_{\min,N}$ between the two global minima of the potential at fixed N. To do this, let p be a path, i.e. a continuous line in configuration space which links the two global minima. For each point of p, the potential takes a value. Since the length of any p is finite, then the set of the differences between the potential along p and the global minimum of the potential at fixed $Nv_{\min,N}$ has a maximum that we will call V_p. Then, we define $B_{\min,N}$ as the infimum of the set of the V_p's associated with all the possible paths p's. We also define the specific minimum barrier $b_{\min,N}=B_{\min,N}/N$.

There is an interesting relation between $b_{\min,N}$ and the thermodynamic critical potential $\langle v\rangle_{\mathrm{c}}$. Let us assume that $\lim_{N\to\infty}b_{\min,N}=b_{\min}$ exists as finite. Then, $\langle v\rangle_{\mathrm{c}}\geqslant b_{\min}+v_{\min}$ holds. This inequality is a consequence of theorem 1 in [14]. Indeed, for $v\in(v_{\min},b_{\min}+v_{\min})$, the $\Sigma_{v,N}$'s are topologically equivalent to the disjointed union of two N-spheres, so that the hypotheses of theorem 1 are satisfied. The implication is that the $\mathbb{Z}_2$ symmetry of the potential is broken for $v\in[v_{\min},b_{\min}+v_{\min})$, whence $\langle v\rangle_c\geqslant b_{\min}+v_{\min}$.

What can we say about $b_{\min}$ as a function of d? Let us start with $d=1$. Suppose the configuration of the system is that of a global minimum, for example, $\phi_i=\sqrt{2J}$, for $i=1,\ldots,N$. Flip a degree of freedom, for example, $\phi_1=-\sqrt{2J}$ to fix the ideas. The potential of the new configuration has increased by the quantity $4J$. Now, continue to flip the nearest neighbors until only one takes the value $\sqrt{2J}$. In so doing, the potential does

J. Stat. Mech. (2024) 073201

not change value. At this point, we flip the last degree of freedom and the potential will return to its global minimum. We have thus described a path in configuration space between the global minima of the potential for which $V_\mathrm{p} = 4J$. Since for $N \to \infty$, the above-defined path is that with the minimum V_p, then the minimum barrier is $B_{\min,N} = 4J$.

For $d = 2$, we can proceed in a similar way as follows. Consider a square lattice with toroidal boundary conditions. Flip the degrees of freedom belonging to a row; then flip the nearest neighbors until all the degrees of freedom are flipped. We have chosen a row (or a column is the same) because it is a path in configuration space of minimum length. Since the lattice is square, then the path length is $N^{1/2}$, so that $B_{\min,N} \propto N^{1/2}$.

For any d, via the same considerations, we can show that $B_{\min,N} \propto N^{(d-1)/d}$. The limiting case $d = \infty$ corresponds to the mean-field case for which we already showed in section 2.2 that $B_{\min,N} \propto N$.

What could the implications of the minimum barrier be on the critical points? The $\Sigma_{v,N}$'s are topologically equivalent to two disjointed N-spheres in the v-interval comprised between $v_{\min,N}$ and the first critical v-level set. Assuming that $b_{\min,N}$ is the value of the minimum barrier implies that the $\Sigma_{v,N}$ corresponding to the potential $v_{\min,N} + b_{\min,N}$ is critical. If $b_{\min,N} \to 0$ in the thermodynamic limit, at least a critical point exists whose critical v-value tends to $v_{\min}$. This means that the interval $(v_{\min,N}, 0)$ cannot be void of critical points, at least from a certain N-value. In section 4.2.1, we see that the considerations above are compatible with the results obtained using the NPHC method.

It is worth noticing that this is strictly related to the convexity properties of the graphic of the configurational microcanonical entropy in the (m, v)-plane. The fact that $b_{\min,N} \to 0$ in the thermodynamic limit makes it possible to divide the system configuration into at least two domains with independently oriented magnetization. This implies that all the spontaneous magnetization values comprised between the maximum and the minimum are allowed for a fixed temperature. This reflects in a flat entropy as a function of m at fixed v comprised between the maximum and the minimum of the spontaneous magnetization. Basically, the graph is non-strictly concave [19, 27–29].

It is possible to analytically compute, via a computer algebra system, the index of the saddle point $(0, \ldots, 0)$, which grows linearly with N at least for the values investigated here (see figure 11). In the mean-field case, the index of the central saddle is 1 independently on N. This is consistent with the fact the limit for $N \to \infty$ of the minimum barrier $b_{\min}$ is finite in the mean-field case and is vanishing for finite d.

4.2.1. Critical points by the NPHC method. We used the NPHC method [33] to solve equation (34), at least for values of N up to 9 and d up to 3. We chose the following cases to compute:

$$\begin{array}{ll} \mathrm{d} = 1; & \mathrm{N} = 4, 7, 8, 9 \\ \mathrm{d} = 2; & \mathrm{N} = 2 \times 2, 3 \times 3 \; . \\ \mathrm{d} = 3; & \mathrm{N} = 2 \times 2 \times 2 \end{array}$$

The boundary conditions are periodic for the cases with $d = 1$ and are toroidal for the other cases. The coupling J is set to 1 because the solutions of equation (34) for

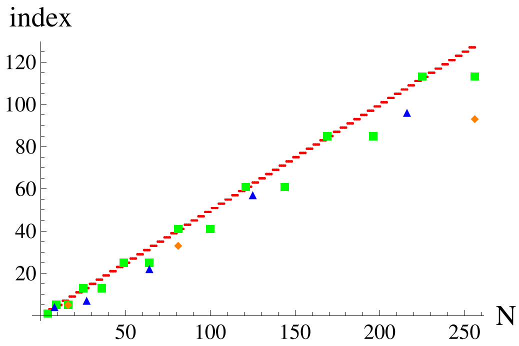

Figure 11. The index of the saddle point $(0,\ldots,0)$ of the model in equation (31) as a function of the number of degrees of freedom for dimension $d=1,2,3,4$ (red points, green squares, blue triangles, orange rhombuses, respectively).

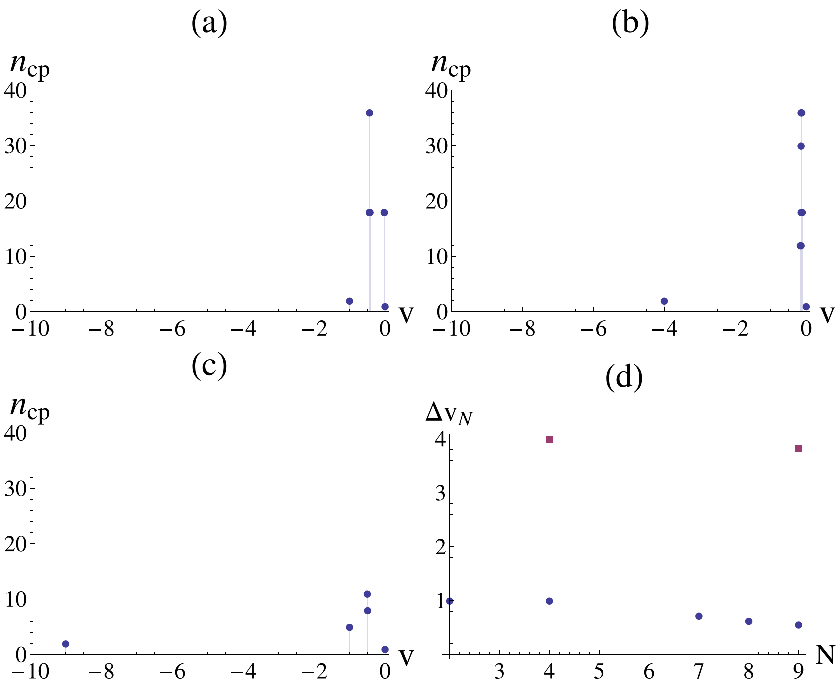

Figure 12. The nearest-neighbors model, equation (31). (a) The number of critical points found by using the NPHC method with respect to their potential density for $d=1$ and $N=9$, (b) for $d=2$ and $N=3\times3$, and (c) for $d=3$ and $N=2\times2\times2$. (d) The difference between the lowest potential critical level above the global minimum and the global minimum for $J=1$ versus N for $d=1$ (disks) and $d=2$ (squares).

any other J' can be obtained by using the scaling law, equation (35). The results are reported in figure 12.

For $d=1$, we found an increasing total number of critical points while increasing N. In particular, at least up to $N=4$, the total number is 3, which are the two global minima and the central saddle. For $N = 7, 8, 9$, the total number is $31, 67, 147$, respectively. The smallness of the computed N-values did not allow us to make a significant statistic, but the data seems compatible with an exponential growth, as in the case of the model in equation (4).

The most interesting feature is that the nearest critical v-level above the global minimum slightly lowers while increasing N (see figure 12(d)). This is a necessary condition if the minimum barrier $B_{\min,N}$ for $d = 1$ is independent of N, as was shown in section 4.2 for a one-dimensional lattice. For a consequence, $b_{\min,N}$ decreases as $1/N$.

For $d = 2$, the total number of critical points is 3 in the lattice 2×2 and some other critical points appear in the lattice 3×3 with total number 165. For $d = 3$, some other critical points, beside the central saddle and the global minima, appear just in the lattice $2 \times 2 \times 2$ with total number 27.

Unfortunately, the computational means at our disposal did not allow us to investigate larger N-values. However, the data found confirm the hypothesis that the shape of the potential cannot be reduced to that of a double well with three critical points, as for the model in equation (3), except in the case mentioned above for very small N-values and for $d = 1, 2$.

4.2.2. On a necessity theorem for PTs. In [12], a theorem on a necessary condition for a PT of Hamiltonian systems was shown. This theorem was already shown in an original version [23], even though it was later falsified by a counterexample [20]. The original theorem, under suitable conditions, established that if the $\Sigma_{v,N}$'s are diffeomorphic for any N in an interval of v-values $[v_0, v_1]$, then the thermodynamic functions have to be analytic at least up to the second order in the same interval. As a consequence, if a PT of the first or second order occurs at $\langle v \rangle_c$, then at least a critical $\Sigma_{v,N}$, with $v \to \langle v \rangle_c$ for $N \to \infty$, exists. Basically, a topological change has to occur as the $\Sigma_{v,N}$ crosses the critical potential. The corrected version of the theorem includes the hypothesis of *asymptotic diffeomorphicity* beside that of diffeomorphicity of the $\Sigma_{v,N}$'s in the interval $[v_0, v_1]$.

Here, we suggest future investigations to understand if the picture of PTs based on the framework of dumbbell-shaped $\Sigma_{v,N}$'s (picture 1, for simplicity) put forward in [16], here applied to the simplified ϕ^4 model, has some convergence with the picture depicted by the aforementioned theorem (picture 2), in particular, with the concept of asymptotic diffeomorphicity. In picture 1, a PT is meant as a $\mathbb{Z}_2$-SBPT, whereas in picture 2, a PT is meant as a loss of analyticity of the thermodynamic functions. These two phenomena are often associated, but some exceptions exist. In picture 1, a necessary and sufficient condition for a $\mathbb{Z}_2$-SBPT was given, whereas in picture 2, the condition for a PT is only necessary. The condition of picture 1 applies only to $\mathbb{Z}_2$-symmetric systems, whereas the aforementioned theorem applies only to finite-range systems, regardless of their symmetries.

To fix the ideas, consider the simplified ϕ^4 model, equation (31), with short-range interaction in two dimensions. The critical potential is always positive, so that the $\mathbb{Z}_2$-SBPT is located in an interval of v-values void of critical points and no topological change located at the critical potential occurs. Regardless, to some extent, a topological change can be restored in the limit $N \to \infty$, as depicted in figure 3 in [16]. In the

J. Stat. Mech. (2024) 073201

broken phase, the $\Sigma_{v,N}$'s are dumbbell-shaped and diffeomorphic to an N-sphere. Since as $N \to \infty$, the volume of the two lobes becomes bigger and bigger with respect to the neck, in non-rigorous terms, we can say that the 'limiting topology' of a sequence of dumbbell-shaped $\Sigma_{v,N}$'s is not equivalent to that of the $\Sigma_{v,N}$'s themselves for each N. In particular, they become topologically equivalent to two N-spheres. In these terms, we can say that a topological change is exactly located at the critical potential in the limit $N \to \infty$. This could have something in common with the concept of asymptotic diffeomorphicity, which contemplates that a topological change can occur in the limit $N \to \infty$. We are aware that speaking of topology in the limit $N \to \infty$ is only a colloquial abstraction because no configuration space survives in that limit.

5. Conclusions

In this paper, we show how a vanishing quadratic term of the local potential of the on-lattice mean-field ϕ^4 model with a $\mathbb{Z}_2$ $(O(1))$ symmetry entails a tragic simplification of the structure of the potential energy landscape. In particular, the number of critical points decreases to three. This has no influence on the $\mathbb{Z}_2$-SBPT properties, so that it makes the general study of the link between the geometry and topology of the potential landscape and the PT easier. The only two critical levels of the potential are located at zero and at the global minimum.

The thermodynamic critical potential of the $\mathbb{Z}_2$-SBPT is located above zero for any value of the coupling constant J. This clearly shows that the $\mathbb{Z}_2$-SBPT is not directly related to the presence of critical points, but rather to a particular shape of the equipotential surfaces $\Sigma_{v,N}$'s, which can been defined as dumbbell-shaped which, in turn, can be entailed by the presence of a double-well potential with a minimum barrier that is proportional to the number of degrees of freedom N. The last property explains the irreducible presence of three critical points because they are the minimum number requested for the occurrence of a double well in an analytic potential.

The short-range case was also investigated. The number of critical points cannot be reduced to three and no topology drastic simplification of the equipotential surfaces $\Sigma_{v,N}$'s can occur. For N-values up to 9 and up to $d = 3$, the presence of critical points, in addition to the two global minima and the central saddle point $(0,\ldots,0)$, was detected using the NPHC method. Incrementing J at fixed N cannot cause any reduction of the number of critical points because a scaling law entails that their number does not change while varying J. The presence of critical points in addition to the global minima and the central saddle can be inferred using thermodynamic reasons. In particular, the short-range interaction causes a minimum potential barrier between the two wells decreasing as $N^{-1/2}$, so that the v-interval between the global minimum and 0 cannot be void of critical points. This means that the $\Sigma_{v,N}$'s cannot be homeomorphic to two disjointed N-spheres above the global minimum, except for a v-interval with $v \to 0$ in the thermodynamic limit.

A future plan is to extend this research to other symmetry groups.

J. Stat. Mech. (2024) 073201

Acknowledgments

I warmly thank Dhagash Mehta for having suggested the application of the NPHC method to the topic of this paper and for having carried out the numerical computations needed to detect the critical points of the short-range cases of the simplified ϕ^4 model included in section 4.2.1. I also warmly thank Marco Pettini for an introduction to the Monte Carlo method and for invaluable discussions.

References

[1] Casetti L, Cohen E G D and Pettini M 2000 Geometric approach to Hamiltonian dynamics and statistical mechanics *Phys. Rep.* **337** 237

[2] Casetti L, Cohen E D G and Pettini M 2002 Exact result on topology and phase transitions at any finite N *Phys. Rev.* E **65** 036112

[3] Franzosi R, Casetti L, Spinelli L and Pettini M 1999 Topological aspects of geometrical signatures of phase transitions *Phys. Rev.* E **60** R5009

[4] Casetti L and Kastner M 2006 Nonanalyticities of entropy functions of finite and infinite systems *Phys. Rev. Lett.* **97** 100602

[5] Casetti L, Kastner M and Nerattini R 2009 Kinetic energy and microcanonical nonanalyticities in finite and infinite systems *J. Stat. Mech.* 07036

[6] Mehta D, Hauenstein J D and Kastner M 2012 Energy-landscape analysis of the two-dimensional nearest-neighbor ϕ^4 model *Phys. Rev.* E **85** 061103

[7] Baroni F 2011 A simple topological model with continuous phase transition *J. Stat. Mech.* 08010

[8] Baroni F 2020 The mechanism of $\mathbb{Z}_2$ symmetry-breaking phase transitions highlighted by an elementary model (arXiv:2006.13734)

[9] Ribeiro Teixeira A C and Stariolo D A 2004 Topological hypothesis on phase transitions: the simplest case *Phys. Rev.* E **70** 016113

[10] Kastner M, Schnetz O and Schreiber S 2008 Nonanalyticities of the entropy induced by saddle points of the potential energy landscape *J. Stat. Mech.* 04025

[11] Di Cairano L 2022 The geometric theory of phase transitions *J. Phys. A: Math. Theor.* **55** 27LT01

[12] Gori M, Franzosi R, Pettini G and Pettini M 2022 Topological theory of phase transitions *J. Phys. A: Math. Theor.* **55** 375002

[13] Andronico A, Angelani L, Ruocco G and Zamponi F 2004 Topological properties of the mean-field ϕ^4 model *Phys. Rev.* E **70** 041101

[14] Baroni F and Casetti L 2006 Topological conditions for discrete symmetry breaking and phase transitions *J. Phys. A: Math. Gen.* **39** 529545

[15] Baroni F 2019 Topology of configuration space of the mean-field ϕ^4 model by Morse theory *Phys. Rev.* E **100** 012124

[16] Baroni F 2020 Necessary and sufficient conditions for $\mathbb{Z}_2$-symmetry-breaking phase transitions *J. Stat. Mech.* 103202

[17] Garanin D A, Schilling R and Scala A 2004 Saddle index properties, singular topology and its relation to thermodynamic singularities for a ϕ^4 mean-field model *Phys. Rev.* E **70** 036125

[18] Hahn I and Kastner M 2006 Application of large deviation theory to the mean-field ϕ^4-model *Eur. Phys. J.* B **50** 311314

[19] Hahn I and Kastner M 2005 The mean-field ϕ^4 model: entropy, analyticity and configuration space topology *Phys. Rev.* E **72** 056134

[20] Kastner M and Mehta D 2011 Phase transitions detached from stationary points of the energy landscape *Phys. Rev. Lett.* **107** 160602

[21] Kastner M 2006 When topology triggers a phase transition *Physica* A **365** 128–31

[22] Gori M, Franzosi R and Pettini M 2018 Topological origin of phase transitions in the absence of critical points of the energy landscape *J. Stat. Mech.* 093204

[23] Pettini M 2007 *Geometry and Topology in Hamiltonian Dynamics and Statistical Mechanics* (Springer)

[24] Wilson K G and Kogut J 1974 The renormalization group and the ϵ expansion *Phys. Rep.* **12** 75

[25] Dauxois T, Lepri S and Ruffo S 2003 Clustering and ensembles inequivalence in the ϕ^4 and ϕ^6 mean-field Hamiltonian models *Commun. Nonlinear Sci. Numer. Simul.* **8** 375–87
[26] Goldenfeld N 1992 *Lectures on Phase Transitions and the Renormalization Group* (Perseusn Publishing)
[27] Lanford O E 1973 *Entropy and Equilibrium States in Classical Statistical Mechanics* (*Statistical Mechanics and Mathematical Problems. Lecture Notes in Physics* vol 20), ed A Lenard (Springer)
[28] Gallavotti G 1999 *Statistical Mechanics. A Short Treatise* (Springer)
[29] Kastner M 2002 Existence and order of the phase transition of the Ising model with fixed magnetization *J. Stat. Phys.* **109** 133–42
[30] Milnor J 1963 *Morse Theory* (Princeton University Press)
[31] Baroni F 2020 Models with symmetry-breaking phase transitions triggered by dumbbell-shaped equipotential surfaces *Phys. Rev.* E **102** 012119
[32] Baroni F 2020 Symmetry breaking phase transitions in mean-field models triggered by double-well potentials *Eur. Phys. J.* B **93** 45
[33] Mehta D 2011 Finding all the stationary points of a potential-energy landscape via numerical polynomial-homotopy-continuation method *Phys. Rev.* E **84** 025702(R)

https://doi.org/10.1088/1742-5468/ad5437